Sequence of Four Orthogonal Smectic Phases in an Achiral Bent-Core Liquid Crystal: Evidence for the SmAP_α Phase

Y. P. Panarin,[1,2] M. Nagaraj,[1] S. Sreenilayam,[2] J. K. Vij,[1,*] A. Lehmann,[3] and C. Tschierske[3]

[1]*Department of Electronic and Electrical Engineering, Trinity College, University of Dublin, Dublin 2, Ireland*
[2]*School of Electronic & Communication Engineering, Dublin Institute of Technology, Dublin, Ireland*
[3]*Institute of Chemistry, Organic Chemistry, Martin-Luther-University Halle-Wittenberg, D06120, Germany*

(Received 30 June 2011; published 7 December 2011)

The mesomorphic properties of an achiral bent-core liquid crystal derived from 4-cyanoresorcinol are studied by polarizing optical microscopy, x-ray diffraction, and second harmonic electro-optic response. It shows a novel sequence of four nontilted or orthogonal smectic phases on cooling: SmA-SmAP_R-SmAP_X-SmAP_A. Here SmAP_X is the new orthogonal polar uniaxial smectic phase. The electric-field-induced transformations in the SmAP_X phase give rise to two biaxial states separated by a uniaxial one. The second harmonic electro-optic response in this phase is interpreted in terms of the polar interaction with the electric field. A comparison of the experimental results with the next-nearest-neighbor model for the structure of the SmAP_X phase shows it to be an SmAP_α phase.

DOI: 10.1103/PhysRevLett.107.247801 PACS numbers: 61.30.Gd, 77.84.−s, 83.80.Xz, 42.65.Ky

The myriad of phases exhibited by bent-core liquid crystals, ferroelectric switching in achiral smectic liquid crystals and the potential for applications have motivated researchers to synthesize new bent-core compounds and to investigate them in detail [1]. Unlike calamitic liquid crystals, the bent-core compounds exhibit a rich variety of orthogonal smectic phases, such as SmAP_A [2–5], SmAP_R [6,7], and SmAP_{AR} [8]. In all these phases, the molecular rotation around its principal axis within a smectic layer is biased at least to some extent. The common characteristic of these phases is that these are nontilted and possess a long-range (or short range in case of SmAP_R) in-layer polarization. This is due to the packing of the molecules along a preferred bent direction which leads to a lining up of the vectors of the molecular dipole moments which are directed along the bent-direction parallel to the layer planes. This is referred to as the ''in-layer polarization direction'' throughout this Letter. In the SmAP_R phase, the in-layer polarization directions in adjacent layers are randomized leading to a macroscopically uniaxial phase and in the SmAP_A phase, they are antiparallel to each other giving rise to an antiferroelectric phase which is biaxial. Recently, a biaxial ferroelectric phase with the in-layer polarization directions parallel to each other in adjacent layers has been observed as a stable ground-state structure (SmAP_F) [9].

Field-induced SmAP_F states can be obtained from the SmAP_A and SmAP_R phases under sufficiently strong electric fields applied parallel to the smectic layers, after the initial randomly distributed (SmAP_R) or antiferroelectrically arranged (SmAP_A) in-layer polarization directions become aligned in the direction of the electric field. Remarkably, in some materials, the transition from SmAP_A to SmAP_F goes through an intermediate uniaxial state appearing as dark texture in a homeotropic cell between crossed polarizers [10]. Hence, the SmAP_A and SmAP_R phases are of interest due to their potential for application in the next generation of fast switching displays [11,12] as well as to advancing the understanding of their internal structures and establishing molecular structure-property relationships [13]. Recently, another randomized polar smectic phase, assigned as SmAP_{AR}, has been observed in a bent-core compound containing a 3-aminophenol-derived central unit [8]. It was suggested that this phase consists of randomly aligned domains of local antiferroelectric order and its stability was attributed to a nonsymmetric molecular architecture containing intermolecular hydrogen bonding.

Here we report mesomorphic properties of a new 4-cyanoresorcinol bisbenzoate compound (PAL30) whose structure is given below, by polarizing optical microscopy (POM), x-ray diffraction (XRD) and electro-optics. This compound exhibits a unique sequence of four orthogonal smectic phases with the phase transitions: isotropic liquid 164 °C [7.9] → SmA 111 °C [0.7] → SmAP_R 108 °C [<0.01] → SmAP_X 91 °C [<0.01] → SmAP_A 38 °C [37.2] → Cryst (observed on cooling, the enthalpy values in kJ mol^{-1} given in square brackets were measured using DSC at 10 K min^{-1} cooling rate). This is the largest number of different orthogonal smectic phases observed so far in a temperature induced phase sequence of a single compound. The low but measurable enthalpy of the SmA to SmAP_R transition can be explained on the basis that the polar layers are formed at this transition, and the absence of a measurable enthalpy for the SmAP_R to SmAP_X and the SmAP_X to SmAP_A transitions can be explained as the latter are only due to changes of the azimuthal in-layer polarization vectors. In this phase sequence, SmAP_X is a new orthogonal polar smectic phase and herein a detailed investigation of this phase is presented. The SmAP_X phase

appears between the SmAP_R and SmAP_A phases, it is optically uniaxial and exhibits a double current peak per half cycle of the applied triangular voltage signal. This phase is distinguishable from SmAP_R phase through the nature of the current response (only a single peak in SmAP_R, a double peak in SmAP_X) and dielectric spectroscopy. The static dielectric permittivity is observed to drop at the SmAP_R-SmAP_X transition temperature. The experimental data are analyzed and compared with the results from simulations that used the next-nearest-neighbor (NNN) model. This comparison shows that the SmAP_X phase represents the SmAP_α phase with the azimuthal angles of successive layers in the range $90° < \varphi < 180°$.

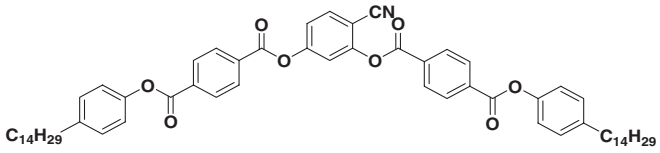

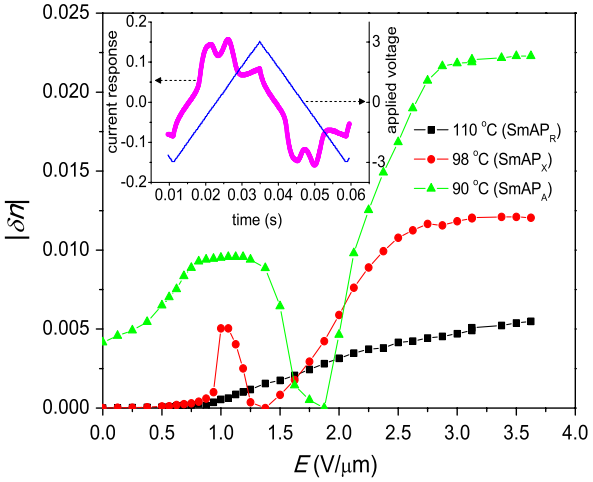

FIG. 1 (color online). Electric field dependent magnitude of biaxiality in SmAP_R (■), SmAP_X (●), SmAP_A (▲) phases. Inset: Current response in SmAP_X (●) phase (in arbitrary units) of PAL30.

The nontilted nature of the smectic phases is confirmed by 2D XRD of a surface aligned sample. The XRD shows sharp layer reflections (layer spacing, $d = 5.6$ nm at 140 °C and 5.8 nm at 70 °C; molecular length $L = 6.5$ nm in the most stretched conformation). In all LC phases these reflections are observed in a direction normal to the line joining the maxima of the diffuse wide angle scattering at $d = 0.48$ nm. The latter scattering remains diffused in the four smectic phases, this excludes the onset of any positional in-plane order. On the average orthogonal organization of the molecules with respect to the layers in all four LC phases is additionally confirmed by optical investigations. For POM and electro-optic studies, homeotropic alignment is obtained by coating the substrates with AL60702 (JSR Korea). A planar alignment is achieved by coating the substrates with RN1175 (Nissan Chemicals Japan) polymer alignment layer. In order to apply an in-plane electric field in a homeotropic cell, indium tin oxide (ITO) electrodes of the bottom substrate are etched with a gap of 80 μm. Figure 1 shows the magnitude of biaxiality, $|\delta n|$ (measured in a homeotropic cell of thickness = 7 μm) of PAL30 in the SmAP_R, SmAP_A and SmAP_X phases against the electric field E applied along the layers.

In the SmAP_R phase (110 °C), the sample is found to be uniaxial and the texture appears dark between the crossed polarizers. Since the in-layer polarization directions are randomly distributed in the absence of an electric field and the primary director (along the average molecular long axes) is orthogonal to the smectic layer plane, the SmAP_R phase [6,7] is macroscopically uniaxial. Application of an electric field disturbs this random distribution of the molecular transverse dipoles and therefore induces in-layer polarization and optical biaxiality. This process obeys Langevin formalism [6] and the value of induced biaxiality increases with lowering temperature. In the SmAP_A phase (90 °C) the sample is biaxial and exhibits a characteristic Schlieren texture for $E = 0$. Application of an in-plane electric field aligns the in-layer polarization directions to give a uniform biaxial antiferroelectric structure with negative (i.e., perpendicular to the electric field) biaxiality, $\delta n_{\mathrm{AF}} \approx 0.01$. A further increase in E causes a transformation to a dark uniaxial intermediate state. In this uniaxial state, the in-layer polarization directions in adjacent layers are perpendicular to each other [10]. Increasing E, transforms the uniaxial dark state into a bright biaxial ferroelectric state with a positive $\delta n_{\mathrm{F}} = 0.022$. In the high temperature range of the SmAP_A phase, $|\delta n_{\mathrm{AF}}|$ is lower than $|\delta n_{\mathrm{F}}|$. With a reduction in temperature, the biaxiality $|\delta n_{\mathrm{AF}}|$ increases faster than $|\delta n_{\mathrm{F}}|$ and finally, $|\delta n_{\mathrm{AF}}| = |\delta n_{\mathrm{F}}|$ [10]. The subscripts AF and F refer to the antiferroelectric and ferroelectric states, respectively.

When the sample is cooled down from the SmAP_R to the SmAP_X phase, it stays perfectly dark (uniaxial) for an applied in-plane electric field up to ~0.95 V/μm. But when E is increased to ~1 V/μm, it transforms to a bright (biaxial) state with negative biaxiality of $\delta n = -0.005$. On a further increase in the field to 1.35 V/μm, this biaxial state becomes dark again. For this uniaxial state, one of the possible explanations is that the in-layer polarizations in neighboring layers are perpendicular to each other. Upon a further increase in E, the uniaxial state again goes to a biaxial one with positive biaxiality and then saturates to a ferroelectric state with $|\delta n_{\mathrm{F}}| = 0.012$. Hence, with increasing field, the SmAP_X phase, exhibits two macroscopically biaxial bright states with opposite signs of biaxiality; these are separated by a uniaxial dark state. The polarization reversal current response of SmAP_X in a planar cell (thickness = 7 μm, frequency = 50 Hz) shows two peaks per half cycle of the applied triangular wave field in the entire temperature range of this phase

[Fig. 1 inset]; this indicates the antiferroelectric nature of the SmAP_X phase. The electro-optic response [14] is studied by inputting the transmittance from a homeotropic cell to a photodiode, the output of which is fed to a lock-in amplifier; its reference signal is drawn from the generator which applies a voltage signal across the in-plane electrodes at a frequency of 110 Hz. As expected; the compound in the various phases shows no response at the fundamental frequency of the applied field for the reason that both positive and negative states are optically equivalent to each other. Nevertheless during switching, these give rise to a response at the 2nd harmonic frequency (EO_2). The magnitude of this response is proportional to $\sin^2\theta$, where $\theta = \pi\delta n d/\lambda$. For $\theta \ll 1$, the linear dependence of $\delta n(E)$ on E would give a quadratic dependence of EO_2 on E, i.e., $EO_2 \propto E^2$.

Figure 2 presents the electric field dependence of EO_2 in the SmAP_R, SmAP_X, and SmAP_A phases. EO_2 data is fitted to the equation, $EO_2 = k\,E^\gamma$, and the exponent γ is determined (Fig. 2 inset). For lower values of E both SmAP_R and SmAP_X phases give $\gamma = 2$. This implies a linear dependence of $\delta n(E)$ on E for low fields which is due to the polar interaction with E. This is consistent with the Langevin dependence of δn on E in the SmAP_R phase. In the SmAP_A phase, however, the exponent γ shows a cross-over behavior from 2.5 to 3.6, interpreted as due to a combination of polar $(P \cdot E)$ and dielectric $(\Delta\varepsilon \cdot E^2)$ interactions. It should be noted that in the SmAP_X phase the dependence, $\delta n(E)$ on E below the threshold field is also linear, while the value of the induced biaxiality is either zero or is below the resolution of the optical compensator.

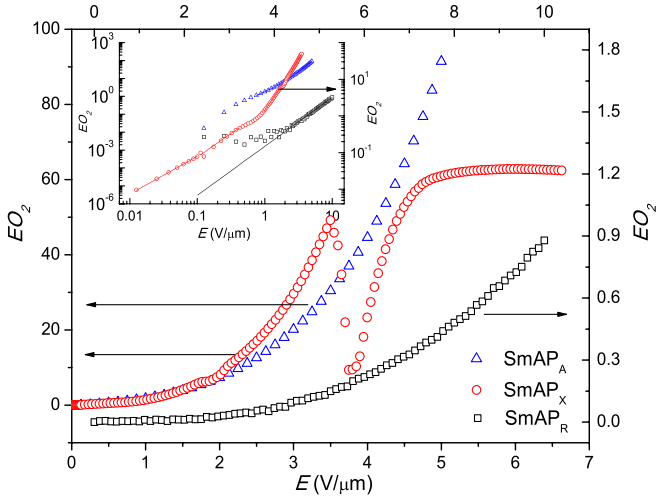

FIG. 2 (color online). Second harmonic electro-optic response (EO_2) in the SmAP_R (□), SmAP_A (△), and SmAP_X (○) phases of PAL30 as a function of E. For SmAP_X, in particular, the low-field response is only considered as for higher fields it transforms to other structures. Inset: A fitting of the EO_2 to $k\,E^\gamma$ on the log-log scale. The exponent is determined from the low field response as for higher fields, phases SmAP_A and SmAP_X transform to the various states.

To theoretically account for the possible structures of the SmAP_X phase, we analyze the free energy as a function of the polarization in a form suggested by Pociecha *et al.* [6] for the nearest neighbor (NN) interactions:

$$G_{\mathrm{NN}} = \sum_j \left[\frac{1}{2}a_1(p_j \cdot p_{j+1}) + \frac{1}{4}b_1(p_j \cdot p_{j+1})^2\right]. \quad (1)$$

For the coefficient of polar interactions $a_1 < 0$ bilinear interlayer interactions favor ferroelectric order due to the van der Waals attractions between the molecules in neighboring layers, whereas for $a_1 > 0$, antiferroelectric order is stabilized by the electrostatic dipolar interlayer interactions. In the SmAP_F and SmAP_A phases, in-layer polarizations in the neighboring smectic layers are parallel and antiparallel, respectively. However the SmAP_F phase was observed as a ground-state structure only for a bent-core compound with two different tails, one of the tails being carbosilane [9]; this is unlikely to be the phase structure applicable here and therefore we consider only $a_1 > 0$.

To identify the possible structures as candidates for the SmAP_X phase, it is necessary either to introduce NN quadrupole interactions [$b_1 \neq 0$, Eq. (1)] [6] or to consider the NNN polar interactions. The coefficient for the quadrupole term $b_1 > 0$ prefers the right angle between in-layer polarization directions in the neighboring smectic layers. The minimization of G_{NN} [Eq. (1)] gives rise to five different structures [6] as shown in Fig. 3. In the three phases, SmAP_α, SmAP_2, and SmAP_R, the magnitude of the angle between the in-layer polarization vectors in the adjacent layers is the same but has the same sign in SmAP_α, opposite sign in SmAP_2, and is randomized in SmAP_R. The phases SmAP_α and SmAP_R are uniaxial whereas SmAP_2 is biaxial. A comparison of the theoretically possible phase sequence with that observed suggests that the structure of the SmAP_X phase may be either SmAP_α or SmAP_2. The SmAP_α phase is uniaxial in the ground state and therefore represents an appropriate structure for the SmAP_X phase. It has a short helical pitch like SmC_α but

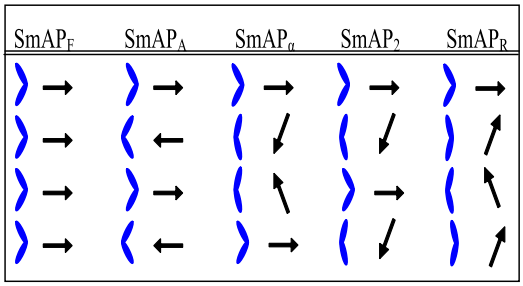

FIG. 3 (color online). Possible structures of orthogonal smectic phases deduced from the minimization of potential G_{NNN}. The bent-core shapes are seen perpendicular to the smectic layer normal; while the in-layer polarization direction seen along the smectic layer normal.

the primary director is not tilted and the helicity arises possibly from flexoelectricity.

The effect of the electric field on the structure was studied by adding the term $-p_j \cdot E$ into Eq. (1). According to this model, these three additional phases have the same free energy G_{NN} in the absence of E and therefore are equally probable, while for $E \neq 0$, SmAP_2 becomes more stable than the other two. Curve 1 in Fig. 4 presents the electric field dependence of the macroscopic spontaneous polarization (normalized to 100%) obtained for $a_1 = 1$, $b_1 = 2$ and $p = 1$ (SmAP_2 case). With these parameters, the magnitude of the angle between the in-layer polarization vectors of the neighboring smectic layers for $E = 0$ is $\sim 120°$ which corresponds to $P_s = 50\%$ in the SmAP_2 phase and saturates for $E = 6$. This also means that for small but $E \neq 0$, the structure should be biaxial but this is not observed experimentally here.

As mentioned above, the SmAP_α structure can also be obtained from the free energy by excluding the quadratic term $(p_j \cdot p_{j+1})^2$ $(b_1 = 0)$ but taking into account the NNN interactions $a_2(p_j \cdot p_{j+2})$ and taking $a_1 < 4|a_2|$. Nevertheless in this case ($a_1 = 2$, a_2 and $b_1 = 0$) the macroscopic polarization shows linear dependence with electric field and saturates for $E = 2$ as shown in curve 2, Fig. 4. Both the linear dependence and the absence of a threshold shown by this curve are not observed experimentally either. Hence, we include in the model the NNN interactions as well as keep b_1 finite and include the interaction term with E. Hence the free energy G_{NNN} becomes

$$G_{\mathrm{NNN}} = \sum_j \Big[\frac{1}{2} a_1 (p_j \cdot p_{j+1}) + \frac{1}{4} b_1 (p_j \cdot p_{j+1})^2 + \frac{1}{2} a_2 (p_j \cdot p_{j+2}) - p_j \cdot E \Big]. \quad (2)$$

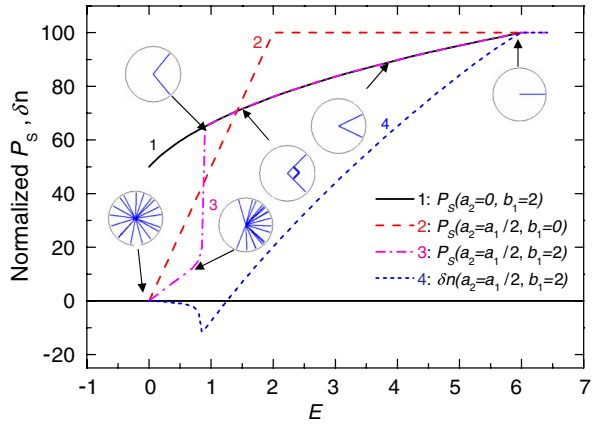

FIG. 4 (color online). Electric-field-induced macroscopic polarization in SmAP_X for different values of parameters a_2 and b_1 (curves 1–3) and induced biaxiality δn (curve 4). The blue lines in the circles related to curve 3 show the distribution of the in-layer polarization vectors in 18 successive smectic layers.

According to Eq. (2), for $a_1 > 0$ (practical relevant case) and for $E = 0$ the SmAP_α structure is found to be more stable than SmAP_2 and therefore the former is the appropriate ground-state structure. For $E > E_{\mathrm{th}}$, where E_{th} is the threshold field, the transition from the uniaxial SmAP_α phase to the biaxial SmAP_2 phase occurs. This is shown in curve 3 of Fig. 4 for the following parameters: $b_1 = 2$, $a_2 = a_1/2$.

Parameter a_2 affects E_{th} for the SmAP_α-SmAP_2 transition but not the saturation field. Curve 3 shows a linear dependence of P_s below the threshold up to $\sim 15\%$, then jumps sharply to $\sim 60\%$ corresponding to the transition SmAP_α-SmAP_2 and then gradually increases to the saturated value for $E = 6$. Remarkably, curve 3 is qualitatively identical to the field-induced apparent tilt angle observed experimentally for SmC_α (Fig. 3(b) in Ref. [15]) except that the tilt angle here is zero. Hence the ground-state structure of SmAP_X is that of the SmAP_α phase. Curve 4 in Fig. 4 is the induced biaxiality (δn) corresponding to curve 3. This curve is in good agreement with the experimental dependence of δn on E in the SmAP_X phase as shown in Fig. 1. For $E < E_{\mathrm{th}}$ it shows very small but linear increase of the induced δn on E. This is in agreement with the quadratic dependence of the EO_2 response observed experimentally (Fig. 2 and the corresponding text). For $E = E_{\mathrm{th}}$, it jumps to the negative value of $\sim 15\%$ and then shows a gradual increase through $\delta n = 0$ (uniaxial state observed experimentally, Fig. 1) to the saturated ferroelectric state with $\delta n = 100\%$.

In conclusion, we have investigated a new bent-core compound and observed an unusual and unprecedented phase sequence of four different orthogonal smectic liquid crystalline phases (SmA-SmAP_R-SmAP_X-SmAP_A) by POM, XRD, 2nd harmonic electro-optic response and the measurements of the polarization reversal current. Among these phases, a new orthogonal smectic phase (SmAP_X) is identified. Electric-field-induced transformations in the SmAP_X phase give rise to a transition from the uniaxial ground state to two biaxial states separated by a field-induced intermediate uniaxial one. The structure and properties of the SmAP_X phase are modeled theoretically by the NNN. Based on a comparison of the experimental results with those from the model, we conclude that the ground-state structure is of SmAP_α phase. In this phase, the in-layer polarization direction rotates from layer to layer with a fixed angle varying in the range $90° < \varphi < 180°$ uniformly between the adjacent layers, similar to the tilt director in a SmC_α phase [15]. Under the influence of an electric field, it undergoes phase transitions first to the SmAP_2 state at E_{th} and then to the SmAP_F state at the saturation voltage. It should be noted that both, SmC_α [15] and SmAP_X, have similar switching current responses. The uniaxial and antiferroelectrically switching SmAP_{AR} phase which appeared between the columnar and isotropic phases [8] could also possibly have SmAP_α structure as is found here.

The authors thank M. Prehm for x-ray investigations and M. Cepic for useful discussions. This work was funded by EU FP7-216025 BIND and SFI RFP 06/RFP/ENE039.

*jvij@tcd.ie

[1] T. Niori, T. Sekine, J. Watanabe, T. Furukawa and H. Takezoe, J. Mater. Chem. **6**, 1231 (1996); R. A. Reddy and C. Tschierske, J. Mater. Chem. **16**, 907 (2006); H. Takezoe and Y. Takanishi, Jpn. J. Appl. Phys. **45**, 597 (2006).

[2] A. Eremin, S. Diele, G. Pelzl, H. Nadasi, W. Weissflog, J. Salfetnikova, and H. Kresse, Phys. Rev. E **64**, 051707 (2001).

[3] B. K. Sadashiva, R. A. Reddy, R. Pratibha, and N. V. Madhusudana, J. Mater. Chem. **12**, 943 (2002).

[4] M. W. Schröder, S. Diele, N. Pancenko, W. Weissflog, and G. Pelzl, J. Mater. Chem. **12**, 1331 (2002).

[5] H. N. S. Murthy and B. K. Sadashiva, Liq. Cryst. **31**, 567 (2004).

[6] D. Pociecha, M. Cepic, E. Gorecka, and J. Mieczkowski, Phys. Rev. Lett. **91**, 185501 (2003).

[7] Y. Shimbo, E. Gorecka, D. Pociecha, F. Araoka, M. Goto, Y. Takanishi, K. Ishikawa, J. Mieczkowski, K. Gomola, and H. Takezoe, Phys. Rev. Lett. **97**, 113901 (2006).

[8] K. Gomola, L. Guo, D. Pociecha, F. Araoka, K. Ishikawa, and H. Takezoe, J. Mater. Chem. **20**, 7944 (2010).

[9] R. A. Reddy, Ch. Zhu, R. Shao, E. Korblova, T. Gong, Yo. Shen, E. Garcia, M. A. Glaser, J. E. Maclennan, D. M. Walba, and N. A. Clark, Science **332**, 72 (2011).

[10] Y. P. Panarin, M. Nagaraj, J. K. Vij, C. Keith, and C. Tschierske, Europhys. Lett. **92**, 26 002 (2010).

[11] Y. Shimbo, Y. Takanishi, K. Ishikawa, E. Gorecka, D. Pociecha, J. Mieczkowski, K. Gomola, and H. Takezoe, Jpn. J. Appl. Phys. **45**, L282 (2006).

[12] M. Nagaraj, Y. P. Panarin, J. K. Vij, C. Keith, and C. Tschierske, Appl. Phys. Lett. **97**, 213505 (2010).

[13] C. Keith, M. Prehm, Y. P. Panarin, J. K. Vij, and C. Tschierske, Chem. Commun. (Cambridge) **46**, 3702 (2010).

[14] Y. P. Panarin, O. Kalinovskaya, and J. K. Vij, Appl. Phys. Lett. **72**, 1667 (1998).

[15] V. Bourny and H. Orihara, Phys. Rev. E **63**, 021703 (2001).